

Sensitivity and Performance Estimates for the Multiple Wavelength, Multiple Incidence Angle Ellipsometry for OCD Applications

Gary Jiang, Michael Kotelyanskii

Presented at the SPIE 2008

INTRODUCTION

New complex transistors architectures⁵ expand application space of the scatterometry beyond measurements of the simple photoresist and a-Si gratings towards characterization of more complex structures. It has been suggested^{3,4}, that in order to achieve that, scatterometry measurements would have to expand beyond the single angle spectroscopic ellipsometry (SE) to include data collected at multiple incidence angles, or sample orientations. We present results of sensitivity and precision estimates studies of periodic lines gratings at multiple incidence angles, different light wave-lengths, and different sample orientations relative to the ellipsometer incidence plane. We consider measurement sensitivity and precision not just for the critical dimensions, but also for the lines profile shapes (middle-, top-, bottom- CD's, top rounding), as well as resolving different elements of the composite spacer layers.

APPLICATIONS AND MODELS

We report sensitivity and precision estimates for three applications, relevant to the manufacturing of the transistor gates structures: ACI – is a a-Si lines array formed after lithography exposure, and etch, and cleaning ADI – photoresist lines after lithography exposure, and photoresist development, and an a-Si gate with the composite spacer (or offset) layers of silicon oxide and nitride around the a-Si gate electrode As shown at Figures 1-3, model parameters include line widths at the top, and at the bottom of the line, position, and width of the narrowest section of the line profile (line waist), and top rounding of the line profile. Top rounding in the model is simplified by a single block at the top of the line with the 45° cut-off at the top corner, and “top rounding” parameter refers to the height of this block

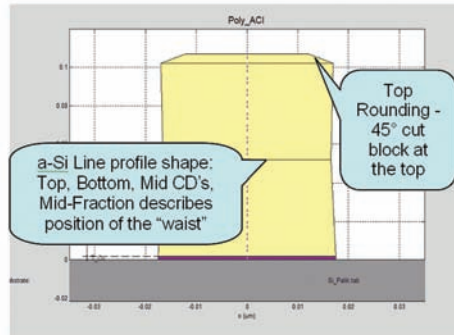


Figure 1 - Structure cross-section model for the a-Si periodic lines array

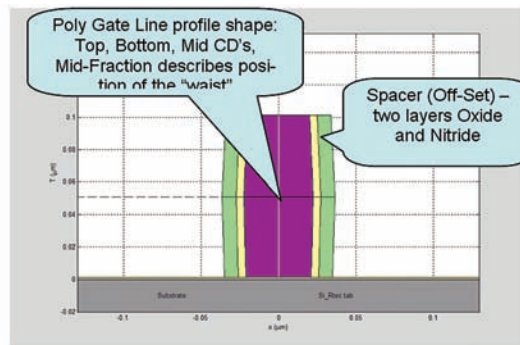


Figure 2 - Structure cross-section model for the a-Si gate with the Si oxide, and Si nitride spacer layers.

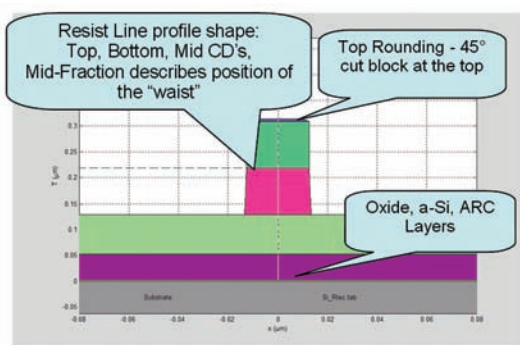


Figure 3 - Structure cross-section model for the photoresist lines grating (ADI)

SENSITIVITY ANALYSIS METHODOLOGY

We discuss measurements performed by the ellipsometer, modulating polarization state of the light passing through the system. If ω is the modulation frequency, measured detector signal consists of the values $\{A_2, B_2, A_4, B_4\}$ representing amplitudes of the modulated signal harmonics at the frequencies 2ω and 4ω .

A “measurement signal” used in the sensitivity analysis and precision estimates for any combination of λ , Ψ , and Φ , is described as the 4-component vector $S\{\lambda, \Psi, \Phi\}$, consisting of the normalized values of $A_2' = A_2/I$, $A_4' = A_4/I$, $B_2' = B_2/I$, $B_4' = B_4/I$, where $I = (A_2^2 + B_2^2 + A_4^2 + B_4^2)^{1/2}$.

MULTI-ANGLE MEASUREMENT SENSITIVITY AT DIFFERENT AZIMUTHS AND WAVELENGTHS

We simulated sensitivities $f_j\{\lambda, \Psi, \Phi\} = \delta S\{\lambda, \Psi, \Phi\} / \delta u_j$ by dividing the change $\delta S\{\lambda, \Psi, \Phi\}$ in response to the independent increments of each of the dimensional parameters u_j of the structure models by the increment value δu_j . Figures 4, 5, and 6 show the sensitivity of multi-angle of incidence measurements at different wavelengths λ , and sample azimuthal orientations Ψ for three applications, described earlier. The value showed on these contour plots is $F\{\lambda, \Psi, \Phi\}_j = f_j\{\lambda, \Psi, \Phi\} / U_j$ with U_j equals 0.3% ($P/T=0.1$) of the target value for the corresponding model parameter. In order to reduce data along the incidence angle dimension Φ , for each pair of λ , and Ψ values, we plot the contours of \log_{10} of the maximal value of the sensitivity $F\{\lambda, \Psi, \Phi\}$ for all the values of Φ . As a benchmark value of the current instruments performance one can assume a typical measured signal variance of today’s systems to be 0.1% or 10⁻³, although it has been suggested that it is reasonable to expect it to go down to 10⁻⁴, or even better with the laser-based systems⁴.

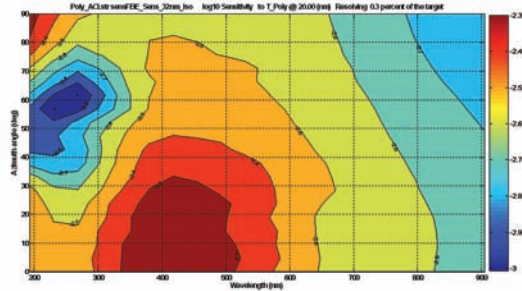


Figure 4a - Sensitivity of the multiple-angle measurement at different λ and Ψ to the line height (T_{Poly}) of the isolated a -Si lines grating. The best sensitivity is at azimuth $\Psi=0^\circ$, for $\lambda \sim 420\text{nm}$, noise level must be 10^{-2.3} or less, in order to resolve change of 0.3% of the target value of the T_{Poly} , if measuring in the range of 350-500nm.

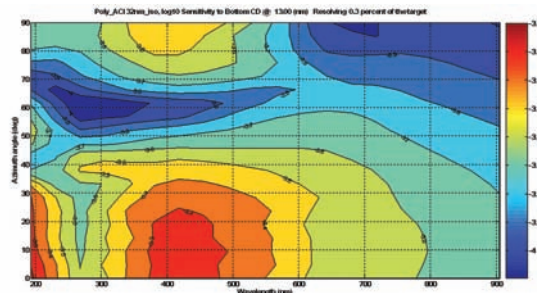


Figure 4b - Sensitivity of the multiple-angle measurement at different λ and Ψ to the Bottom CD of the isolated a -Si lines grating. The best sensitivity is at azimuth $\Psi=0^\circ$, for $\lambda \sim 420\text{nm}$, noise level must be 10^{-3.3} or less, in order to resolve change of 0.3% of the target value of the Bottom CD.

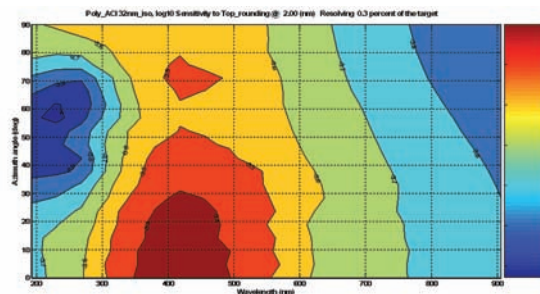


Figure 4c - Sensitivity of the multiple-angle measurement at different Ψ and λ to the Top Rounding of the isolated a -Si lines grating. The best sensitivity is at azimuth $\Psi=0^\circ$, for $\lambda \sim 420\text{nm}$, noise level must be 10^{-3.3} or less, in order to resolve change of 0.3% of the target value of the Top rounding.

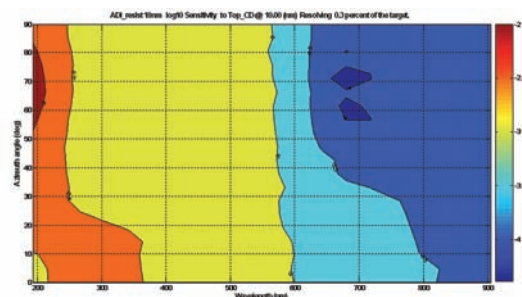


Figure 5a - Sensitivity of the multiple-angle measurement at different λ and Ψ to the top CD of the 18 nm photoresist lines grating. The best sensitivity is at azimuth $\Psi=70^\circ$, for $\lambda \sim 190\text{nm}$, noise level can be 10⁻² or less, in order to resolve change of 0.3% of the target value of the top CD, if measuring in DUV. About 10 \times lower noise levels are required at $\lambda > 300\text{nm}$

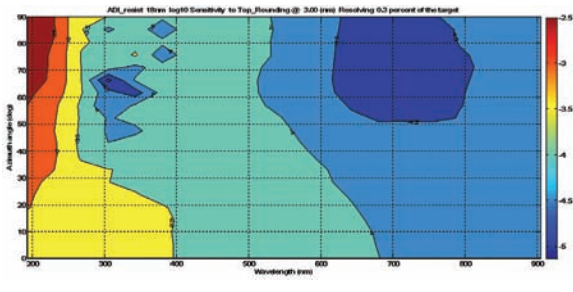


Figure 5b - Sensitivity of the multiple-angle measurement at different λ and Ψ to the Top Rounding of the 18 nm photoresist lines grating. The best sensitivity is at azimuth $\Psi=90^\circ$, for $\lambda\sim 200\text{nm}$, noise level can be 10-2.5 or less, in order to resolve change of 0.3% of the target value of the Top rounding, if measuring in DUV around or below 200 nm.

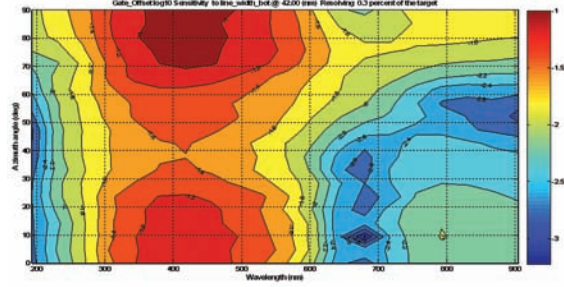


Figure 6c - Sensitivity of the multiple-angle measurement at different λ and Ψ to the bottom line width in the a-Si Gate/Offset application. The best sensitivity is at azimuth $\Psi=90^\circ$, for $\lambda\sim 400\text{nm}$, similar to the a-Si grating, noise level can be 10-1 or less, in order to resolve change of 0.3% of the target value of the bottom line width.

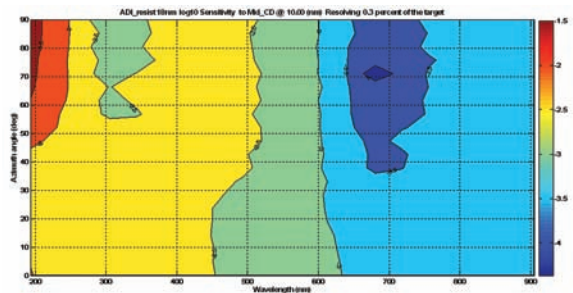


Figure 5c - Sensitivity of the multiple-angle measurement at different λ and Ψ to the middle CD of the 18 nm photoresist lines grating. The best sensitivity is at azimuth $\Psi=90^\circ$, for $\lambda\sim 190\text{nm}$, noise level can be 10-2 or less, in order to resolve change of 0.3% of the target value of the Mid CD, if measuring in DUV.

ESTIMATED PARAMETER PRECISION FOR MULTI-PARAMETER MEASUREMENTS

Figure 7 shows a fairly good comparison of the calculated, and observed precisions for an a-Si grating arrays, when line height, top and bottom critical dimensions are simultaneously extracted, assuming different noise levels for each wavelength, obtained from the actual repeatability measurements, assuming the noise level independent of the incidence angles.

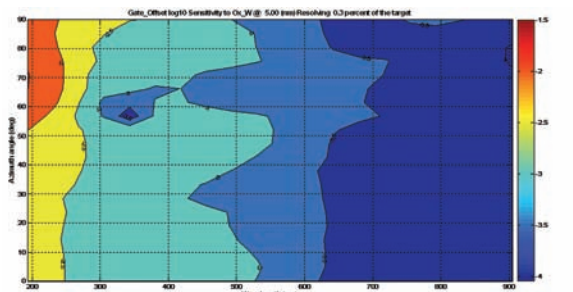


Figure 6a - Sensitivity of the multiple-angle measurement at different λ and Ψ to the thickness of the Si oxide spacer layer in the a-Si Gate/Offset application. The best sensitivity is at azimuth $\Psi=90^\circ$, for $\lambda\sim 190\text{nm}$, noise level can be 10-1.5 or less, in order to resolve change of 0.3% of the target value of the thickness of the Si oxide, measuring in DUV below 300 nm is necessary.

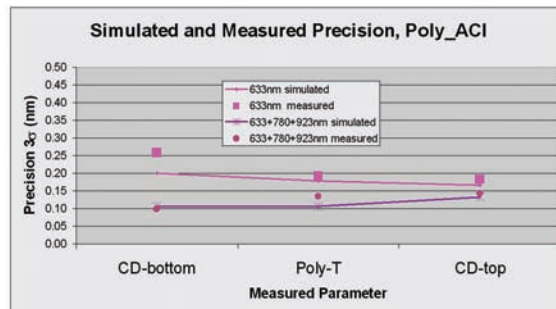


Figure 7 - Measured vs. Predicted parameter precision for Poly_ACI at different orientation

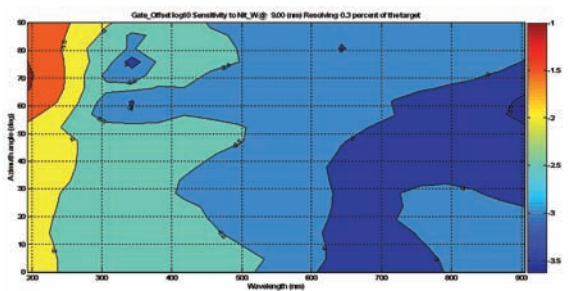


Figure 6b - Sensitivity of the multiple-angle measurement at different λ and Ψ to the width of the Si nitride spacer layer in the a-Si Gate/Offset application. The best sensitivity is at azimuth $\Psi=90^\circ$, for $\lambda\sim 190\text{nm}$, noise level can be 10-1 or less, in order to resolve change of 0.3% of the target value of the Si nitride spacer layer thickness. DUV $\lambda<300\text{ nm}$ is required to resolve this layer.

Tables 1-3 presents estimated precision values for the selected applications, when using angle of incidence range from $\Phi=45^\circ$ to $\Phi=65^\circ$, and combining measurements at few different wavelengths. We report results for a sample azimuthal orientation, providing the best precision estimates, which turns out to be either $\Psi=0^\circ$ or $\Psi=90^\circ$ for all applications considered.

In order to simplify our comparison, and to emphasize the effects of adding the angle resolved measurement to the wavelengths scans, we report estimated parameter precision, divided by the values, estimated for the single angle spectroscopic ellipsometer (SE) at 68° covering wavelengths range from 190 nm to 900 nm with 5 nm resolution, and measuring in the non-conical configuration. Values in the tables reflect relative improvement, compared to the SE performance for the similar application, e.g. value of 0.5 means two times smaller standard deviation, and 2x performance for the multi-angle measurement, while value of 2 would present worse performance, compared to the single angle SE. One has to be cautious trying to extrapolate these results in order to compare performances of the real systems, having different noise levels across the covered spectral range. For instance, using lasers, instead of the UV lamps, at selected wavelengths may significantly enhance photon budget and reduce system noise levels by an order of magnitude or even better⁴.

Application	Model Parameter	Value (nm)	MultiAngle @633,780, 923,405, 266,193 nm	MultiAngle @405, 266, 193 nm	MultiAngle @633,923, 266 nm
ACI a-Si Dense lines (32 nm mode)	Pitch	130	Fixed	Fixed	Fixed
	Bottom CD	13	1.08	1.31	2.85
	T Poly	20	0.55	0.62	1.38
	Mid CD	14	0.58	0.66	2.02
	Top CD	13	0.54	0.56	1.24
	Top Rounding	2	0.73	0.82	1.10
ACI a-Si ISO-lated lines (32 nm mode)	Pitch	360	Fixed	Fixed	Fixed
	Bottom CD	13	0.52	0.50	0.97
	T Poly	20	0.92	0.61	0.99
	Mid CD	14	0.47	0.54	1.36
	Top CD	13	0.38	0.60	1.16
ACI a-Si Dense lines (18 nm mode)	Pitch	70	Fixed	Fixed	Fixed
	Bottom CD	7	0.38	0.38	2.19
	T Poly	20	0.25	0.29	0.79
	Mid CD	7	0.39	0.41	3.61
	Top CD	7	0.47	0.50	4.37
	Top Rounding	1	0.24	0.27	0.92

Table 1 - Target parameter values, and estimated parameter precisions for the multiple wavelengths, multiple incidence angle measurements, divided by the same estimates for the single angle SE, for the etched a-Si gate lines array application, measuring line height, line width at the top, bottom, of the line, and top rounding, simultaneously, while keeping line pitch fixed.

Application	Model Parameter	Value (nm)	MultiAngle @633,780, 923,405, 266,193 nm	MultiAngle @405, 266, 193 nm	MultiAngle @633,923, 266 nm
a-Si Gate/Spacer	Pitch	260	Fixed	Fixed	Fixed
	Bottom CD	42	1.86	1.97	4.92
	Gate_Ox	1	Fixed	Fixed	Fixed
	T Poly	100	1.01	1.29	4.30
	Top CD	40	1.40	1.43	6.84
	Mid CD	45	2.60	2.83	8.77
	Mid-Fraction	1	Fixed	Fixed	Fixed
	Ox Spacer Width	5	0.55	0.61	7.98
Nit Spacer Width	3	0.43	0.45	7.59	

Table 2 - Target parameter values, and estimated parameter precisions for the multiple wavelengths, multiple incidence angle measurements, divided by the same estimates for the single angle SE, for the a-Si Gate/Spacer application, measuring line height, line width at the top, bottom, and middle of the line, and trying to resolve individual Si oxide, and Si nitrite spacer layers thicknesses simultaneously.

Application	Model Parameter	Value (nm)	MultiAngle @633,780, 923,405, 266,193 nm	MultiAngle @405, 266, 193 nm	MultiAngle @633,923, 266 nm
ADI Resist Dense Lines (32 nm)	Pitch	130	Fixed	Fixed	Fixed
	T Resist	120	0.56	0.56	10.94
	T Poly	40	Fixed	Fixed	Fixed
	T Arc	77	Fixed	Fixed	Fixed
	Top Rounding	3	0.54	0.54	11.54
	Top CD	18	1.34	1.35	7.98
	Mid CD	18	1.36	1.36	9.43
	Bot CD	19	1.62	1.65	9.86
ADI Resist Isolated Lines (32 nm)	Pitch	360	Fixed	Fixed	Fixed
	T Resist	120	0.62	0.62	6.13
	T Poly	40	Fixed	Fixed	Fixed
	T Arc	77	Fixed	Fixed	Fixed
	Top Rounding	3	0.56	0.56	6.00
	Top CD	18	1.20	1.20	11.53
	Mid CD	18	1.01	1.01	16.19
	Bot CD	19	1.02	1.03	18.04
ADI Resist Dense Lines (18 nm)	Pitch	70	Fixed	Fixed	Fixed
	T Resist	60	1.10	1.16	6.70
	T Poly	20	Fixed	Fixed	Fixed
	T Arc	77	Fixed	Fixed	Fixed
	Top Rounding	3	0.97	1.03	6.04
	Top CD	10	1.21	1.28	8.42
	Mid CD	10	1.15	1.22	7.38
	Bot CD	11	1.49	1.58	7.84
ADI Resist Isolated Lines (18 nm)	Pitch	200	Fixed	Fixed	Fixed
	T Resist	60	0.82	0.82	5.30
	T Poly	20	Fixed	Fixed	Fixed
	T Arc	77	Fixed	Fixed	Fixed
	Top Rounding	3	0.82	0.83	6.06
	Top CD	10	0.74	0.74	3.57
	Mid CD	10	0.77	0.77	3.18
	Bot CD	11	1.22	1.22	34.06
Mid_Fraction	0.5	0.85	0.85	0.61	

Table 3 - Target parameter values, and estimated parameter precisions for the multiple wavelengths, multiple incidence angle measurements, divided by the same estimates for the single angle SE, for the photoresist lines array after development (ADI), measuring photoresist line height, and profile, expressed as line width at the top, bottom, of the line, top rounding, and position and width of the narrowest line cross-section, simultaneously, while keeping line pitch fixed.

CONCLUSIONS

We have estimated relative performance enhancements of scatterometry measurements employing multiple incidence angles, and sample orientations, for three applications relevant for the manufacturing of the advanced CMOS transistor gate structures.

We find that for all applications, except for some parameters of the 18 nm photoresist lines gratings, the most sensitive measurements occur when lines are either parallel, or orthogonal to the incidence plane of the ellipsometer. This observation is similar to the results reported for the Mueller polarimeter measurements⁷.

Shorter wavelengths are critical for the sensitivity improvement, and better performance when multiple structure parameters are to be determined simultaneously. Sensitivity increases more than order of magnitude for the wavelengths below 200 nm for the photoresist gratings. This sensitivity increase is probably due to the strong increase of the refractive index of the photoresist, and dielectrics in the DUV range. In contrast, in a-Si grating, where the refractive index is already fairly high across the whole wavelength range, its further increase towards the shorter wavelength being off-set by the even stronger light absorption at the shorter wavelengths, leading to the most sensitive wavelength range between 300 nm and 500nm.

Adding multiple incidence angle measurements at a few wavelengths does enhance performance compared to the single angle spectroscopic measurement, provided, that these wavelength cover the high sensitivity range. Using wavelengths in the blue or UV spectral range is much more beneficial, compared to the red and infrared wavelengths. Adding more longer wavelengths outside of the high sensitivity range does not bring much benefit.

REFERENCES

- 1 Niu X.,Jakatdar N., Yedur S., Singh B., "Specular Spectroscopic Profilometry for the Sub-0.18mm PolySi-Gate Processes", Proc.of SPIE, vol.3998 (2000)
- 2 Bunday B., Peterson A., and Allgair J., "Specifications, Methodologies and Results of Evaluation of Optical Critical Dimension Scatterometer Tools at the 90 nm CMOS Technology Node and Beyond". Proceedings of SPIE Microlithography, v5752, pp 304-323, (2005)
- 3 Silver R.,Germer T.,Attota R.,Barnes B.M.,Bunday B.,Allgair J.,Marx E.,Jun J., "Fundamental Limits of Optical Critical Dimension Metrology: A Simulation Study", Metrology, Inspection, and Process Control for Microlithography XXI, edited by Chas N. Archie, Proc. of SPIE Vol. 6518, 65180U, (2007)
- 4 Opsal J., "OPTICAL SCATTEROMETRY: How far can one go with optical metrology?", Laser Focus World, vol. 42, No.9, September, (2006)
- 5 Lammers, D., "Intel Takes 45 nm Process to IEDM", Semiconductor International, December 13, (2007)
- 6 Azzam R. M. A. , Bashara N. M., [Ellipsometry and Polarized Light], 2nd ed., North-Holland, (1986).
- 7 Novikova T., De Martino A., Ben Hatit S., and Drévilon B., "Application of Mueller polarimetry in conical diffraction for critical dimension measurement in microelectronics," Appl. Opt. 45, 3688-3697 (2006).
- 8 International Technology Roadmap for Semiconductors, 2006 Update, (2006) http://www.itrs.net/Links/2006Update/FinalToPost/14_Metrology2006Update.pdf